Synthesis and Characterization of Poly(urethane-benzoxazine)/Clay Hybrid Nanocomposites

Tsutomu Takeichi, Yong Guo

School of Materials Science, Toyohashi University of Technology, Tempaku-cho, Toyohashi 441-8580, Japan

ABSTRACT: Poly(urethane-benzoxazine)/clay hybrid nanocomposites (**PU/Pa–OMMT**s) were prepared from an *in situ* copolymerization of a polyurethane (**PU**) prepolymer and a monofunctional benzoxazine monomer, 3-phenyl-3,4-dihydro-2H-1,3-benzoxazine (**Pa**), in the presence of an organophilic montmorillonite (**OMMT**), by solvent method using DMAc. **OMMT** was made from cation-exchange of Na-montmorillonite (**MMT**) with dodecyl ammonium chloride. The formation of the exfoliated nanocomposite structures of **PU/Pa-OMMT** was confirmed by XRD from the disappearance of the peak due to the basal diffraction of the layer-structured clay found in both **MMT** and **OMMT**. DSC showed that, in the presence of **OMMT**, the curing temperature of **PU/Pa** lowered by ca. 60°C for the onset and ca. 20°C for the maximum. After curing at 190°C for 1 h, the exothermic peak on DSC disappeared. All the obtained films of **PU/Pa–OMMT** were deep yellow and transparent. As the content of **OMMT** increased, both the tensile modulus and strength of **PU/Pa–OMMT** films increased, while the elongation decreased. The characteristics of the **PU/Pa–OMMT** films changed from plastics to elastomers depending on **OMMT** content and **PU/Pa** ratio. **PU/Pa–OMMT** films also exhibited excellent resistance to the solvents such as tetrahydrofuran, *N,N*-dimethylformamide and *N*-methyl-2-pyrrolidinone. The thermal stability of **PU/Pa** were enhanced remarkably even with small amount of **OMMT**. © 2003 Wiley Periodicals, Inc. J Appl Polym Sci 90: 4075–4083, 2003

Key words: polyurethanes; polybenzoxazines; nanocomposites; organoclay

INTRODUCTION

Technological progress is getting more acutely dependent on the state-of-the-art materials that possess quite new or vastly enhanced properties. Individually, few pure polymeric materials embody all of the physical, mechanical, and thermal properties required for a given application. Thus, many materials are mostly used as alloys, blends, and/or composites, which are able to be tailor-made accordingly.[1] One of the most important features of the materials is the possibility of controlling their macroscopic properties by designing their structures at the nanometer level.[2] Recent studies on polymer–clay hybrid nanocomposites have been offering many spectacular approaches to this attractive accomplishment.[3–5] The blossoming out of polymer–clay hybrid nanocomposites as a class of the most rapidly developed modern materials owes to the pioneering works by the group of Toyota Central R&D Labs., Inc., who discovered the possibility to build a nanostructure from nylon 6 and organically modified montmorillonite.[3,6,7] Their newly developed materials showed great improvements of the mechanical properties, barrier properties, and thermal stability at low clay loading due to the high aspect ratio of the clay.

Polymer–clay composites are usually divided into three general classes, namely, conventional composite where the clay acts as a rigid filler, intercalated nanocomposite consisting of a regular insertion of the polymer in between the clay layers, and delaminated (or exfoliated) nanocomposite where ca. 1 nm-thick monolayers are dispersed into the matrix. The last configuration is of particular interest because it makes the entire surface of clay layers available for the polymer, and maximizes polymer–clay interactions. In such an environment, the interfacial bonding between the polymer matrix and the reinforcing materials will be dramatically increased. Thus, polymer–clay hybrid nanocomposites exhibit increased modulus and strength, higher heat distortion temperature, decreased thermal expansion coefficient, lower gas permeability, and superior solvent resistance, compared with the pristine polymer. The investigations on polymer–clay hybrid nanocomposites have been extensively performed with a huge number of polymeric materials, including epoxy resin,[8–10] unsaturated polyester,[11,12] polybenzoxazine,[13,14] polyamide,[6,7,15] polyimide,[16–19] poly(ether-imide),[20] polypropylene,[21–23] poly(styrene-*b*-butadiene),[24] polyurethane (**PU**),[25,26] poly(urethane-urea),[27] poly(methyl methacrylate),[28,29] and poly(ethylene-vinylacetate).[30]

Recently, we reported the synthesis of poly(urethane-benzoxazine) films from **PU** prepolymer and monofunctional or bifunctional benzoxazine mono-

mers, 3-phenyl-3,4- dihydro-2H-1,3-benzoxazine (**Pa**) or bis(3-phenyl-3,4-dihydro-2H-1,3-benzoxazinyl) isopropane (**Ba**), respectively.[31,32] The studies were aiming at the improvement of the thermal stability of **PU** and also the toughness of polybenzoxazine. The films exhibited the characteristics of either plastic or elastomer depending on the ratio of **PU** and polybenzoxazine. Our investigations also revealed that the complete cure of the benzoxazine monomer was hard to accomplish in the presence of **PU**, due to the poor thermal stability of **PU**. Although the heat resistance of **PU** was indeed enhanced by the incorporation of polybenzoxazines, further improvement of the thermal properties could be achieved if a pathway to an efficient cure of benzoxazines is discovered. More recently, we reported the studies on polybenzoxazine–montmorillonite hybrid nanocomposites from **Ba** and organophilic montmorillonite (**OMMT**).[13] Interestingly, in the presence of **OMMT**, the curing temperature of **Ba** was lowered by 30°C, due to the catalysis of the acidic onium protons on the **OMMT** surface. This opens a novel route to an achievement of better curing of benzoxazines at lower temperature. It is therefore worthwhile to investigate the effect of layered clay on the curing behavior of benzoxazine of poly(urethane-benzoxazine). The current study is an extension of our ongoing researches on polymer–clay hybrid nanocomposites.[13,19,33] In this work, we prepared poly(urethane-benzoxazine)/clay hybrid nanocomposites (**PU/Pa–OMMT**)**,** and studied the effect of clay on the preparation and thermomechanical properties of **PU/Pa**.

EXPERIMENTAL

Reagents

Kunipia-F, a Na-montmonrillonite (**MMT**) with cation exchange capacity (CEC) of 119 mEq/100 g, was generously supplied by Kunimine Industry Co. Dodecylamine and conc. hydrochloric acid (35%) was used as received from Tokyo Kasei, Japan. **Pa** was generously supplied by Shikoku Corporation, Japan, and used without further purification. Polyethyleneadipate polyol with molecular weight of 1000 (OH number in KOH; 113) and 2,4-tolylene diisocyanate (TDI) were provided by Nippon Polyurethanes Industry Co. Ltd. TDI, having 99% of purity for 2,4-isomer with an m.p. of 21°C, was used as received. Polyethyleneadipate polyol was dehydrated at 80°C for 10 h under vacuum just before use. All the solvents used in this study were purified according to the standard methods.

Organic modification of MMT

OMMT was prepared by a cation-exchange reaction between Na cation and dodecyl ammonium chloride,

according to the reported methods.[4,19] The procedure of organic modification of **MMT** was carried out as follows. To the suspension of 4.63 g (25.0 mmol) of dodecylamine in 500 mL of distilled water, 2.60 g (25.0 mmol) of conc. HCl was added, and the mixture was stirred at 80°C until it became clear, affording dodecylammonium chloride. To this solution, a suspension of 12.5 g of **MMT** in 500 mL of distilled water was added, and the mixture was mechanically stirred at 80°C for ca. 6 h. The obtained white precipitate was collected by suction filtration and was then poured into hot water (ca. 60°C) followed by stirring for 2 h to remove the salt. This process was repeated several times until no chloride was detected in the filtrate by 0.1 N AgNO$_3$. The resultant was dried in an air-blowing oven at 110°C for 3 days, affording white powder.

Preparation of PU/Pa-OMMT

The procedure for the preparation of **PU/Pa** = 50/50 with 1% **OMMT** will be shown below as an example. An **OMMT** suspension in DMAc was prepared by dispersing 5.701 g of **OMMT** in 100 mL of DMAc at 80°C with stirring until getting stable suspension. The 0.81 g of 5 wt % **OMMT** suspension (40.7 mg of **OMMT**) was mixed with 2.012 g (9.52 mmol) of **Pa** in 6 mL of DMAc followed by stirring at 60°C for 4 h to obtain clear solution. To this solution, 2.013 g (2.03 mmol) of **PU** prepolymer, which was synthesized from TDI and polyethyleneadipate polyol in 2 : 1 molar ratio according to the reported method,[34–36] was then added. After stirring continuously for an additional 1 h, the transparent homogenous solution was cast on glass plates using a doctor blade, and dried at 60°C for 18 h in an air-blowing oven. The cast films were then thermally treated at 100, 150, 170, and 190°C for 1 h each. We also prepared the corresponding pristine poly(urethane-benzoxazine) films for comparison.

Characterizations

IR spectra were obtained using a JASCO spectrophotometer model FT/IR-420. X-ray diffraction (XRD) was observed from an X-ray diffractometer, Rigaku RINT2000 using CuKα radiation and scanning rate of 0.3°/min. Elemental analysis was carried out by Yanaco CHN corder MT-6. Differential scanning calorimetry (DSC) was recorded on Thermo Plus 2 DSC8230 at a heating rate of 10°C/min under nitrogen flow. Thermogravimetric analyses (TGA) were determined with Rigaku Thermo Plus 2 TG-DTA TG8120 at a heating rate of 5°C/min under argon flow. The dynamic viscoelastic measurements were conducted on ORIENTEC Automatic Dynamic Viscoelastomer Rheovibron DDV-01FP with a heating rate of 4°C/min at a frequency of 35 Hz. The tensile properties were
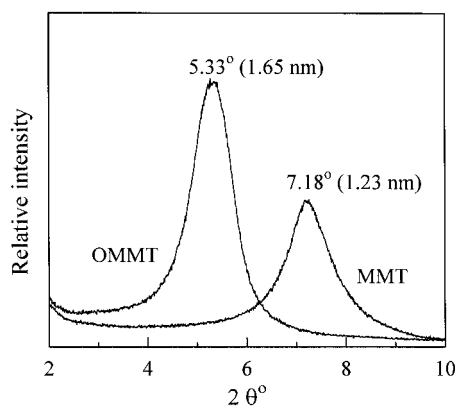
Figure 1 XRD patterns of **MMT** and **OMMT**.

Figure 2 XRD patterns of **PU/Pa**(50/50)-**OMMT** cured at 190°C with **OMMT** loading (a) 1%, (b) 3%, (c) 5%, (d) 7%, (e) 10%, and (f) 20%.

measured on Imada Seisaku-sho Model SV-3 at a crosshead speed of 2 mm/min using 20 mm of the film length. The tensile properties of each sample were determined from the average of at least five tests.

RESULTS AND DISCUSSION

Preparation of PU/Pa-OMMT

Dispersion of clay layers into polymer matrix is a matter of vital importance to obtain polymer–clay nanocomposites. Due to the incompatibility between hydrophobic polymers and hydrophilic pristine **MMT**, the modification of the organophobic **MMT** into organophilic characteristics is a critical stage on the preparation of polymer–clay nanocomposites.[4] In this study, we chose dodecylammonium chloride as the surfactant for the modification. Dodecylamine has 12 carbons, which is necessary to obtain an exfoliated nanocomposites, and is one of the typical modifier of **MMT**.[3,15] Figure 1 shows XRD patterns of **MMT** and **OMMT**. The diffraction peaks of **MMT** and **OMMT** appeared at $2\theta = 7.18°$ and $5.33°$, respectively. The values correspond to the basal spacing (d_{001}) of 1.23 and 1.65 nm, and the gallery height of 0.27 and 0.69 nm, respectively. The enlarged gallery height means that dodecyl ammonium salt was inserted into the galleries of **MMT**, making clay organophilic.
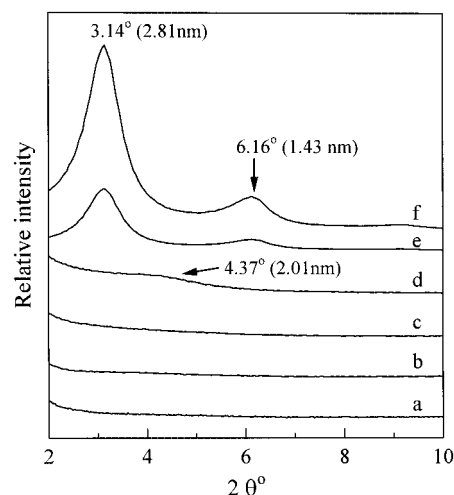
Utilizing **OMMT**, **PU/Pa–OMMT** nanocomposite films were prepared following the compositions given in Table I. **PU/Pa** weight ratios are 20/80, 50/50 80/20, and 90/10 with various **OMMT** content. The thickness of the films was in the range of 0.1–0.2 mm. All the obtained films of **PU/Pa–OMMT** by thermally treating at 190°C were deep yellow and transparent except those with more than 10% of **OMMT**, which were slightly decreasing in apparent clearness.

The structure of the **PU/Pa–OMMT** nanocomposite was observed by XRD measurement. Figure 2 shows XRD patterns of **PU/Pa–OMMT** films obtained by thermal cure at 190°C, for **PU/Pa** = 50/50 (wt ratio) with various **OMMT** content. In the case of **PU/Pa** with **OMMT** loading less than 5% [Fig. 2(a)–(c)], the diffraction peaks found in **MMT** and **OMMT** completely disappeared, indicating that the **OMMT** became disordered and that exfoliated nanocomposite was formed. As the content of **OMMT** increased up to 7%, however, a broad diffraction was slightly observed at around $2\theta = 4.37°$ [Fig. 2(d)], corresponding to $d_{001} = 2.01$ nm (the gallery height of 1.05 nm). At 10% [Fig. 2(e)] and 20% of **OMMT** content [Fig. 2(f)],

TABLE I
The Composition of PU/Pa-OMMT Films[a]

PU/Pa ratio wt (mol)	Amount (g)		OMMT content (mg)						Film[b]
	PU	**Pa**	1%	3%	5%	7%	10%	20%	
20/80 (4/96)	0.671	2.684	33.9	103.8	176.6	252.5	—	—	P
50/50 (14/86)	2.013	2.012	40.7	124.5	211.8	303.0	—	—	P
80/20 (39/61)	3.264	0.816	41.2	126.2	214.7	307.1	453.3	1020.0	E
90/10 (59/41)	3.222	0.358	36.2	110.7	188.4	269.5	397.8	895.0	E

[a] PU was termed as using PU prepolymer; OMMT was used with the suspension of 5 wt% OMMT in DMAc.
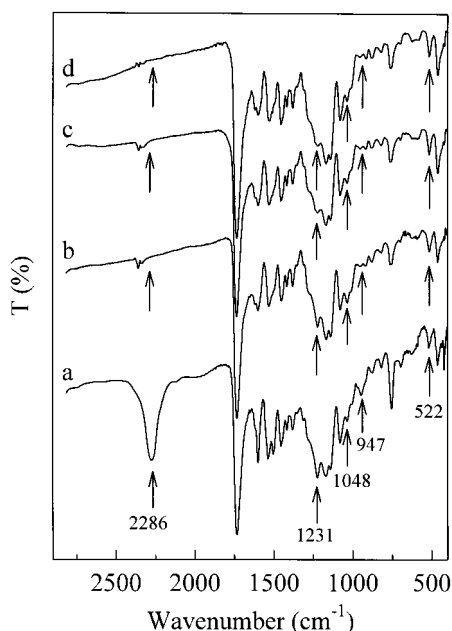[b] P: plastic, E: elastomer.

Figure 3 IR spectra of **PU/Pa**(50/50) with 3% **OMMT**: (a) before cure and cured at: (b) 150°C/1 h, (c) 170°C/1 h, and (d) 190°C/ 1h.

the diffraction peaks evidently appeared at $2\theta = 3.14°$ and $6.16°$, corresponding to $d_{001} = 2.81$ and 1.43 nm, and the gallery height of 1.85 and 0.47 nm, respectively. These results indicate the presence of the aggregated configuration of **OMMT**, which are familiar in the case of high clay loading for the nanocomposites such as polybenzoxazine/clay[13] and poly(urethane-urea)/clay.[27] Similar XRD patterns were observed for **PU/Pa–OMMT** with other **PU/Pa** ratios.

The *in situ* copolymerization of **PU** prepolymer and **Pa** was characterized by IR. Figure 3 shows an example of the IR spectra in the case of **PU/Pa**-50/50 with 3% of **OMMT** after cure at various temperatures. Characteristic absorptions of **Pa** were found for the uncured **PU/Pa** at 1231 cm^{-1} assigned to aromatic carbon–oxygen stretching mode of benzoxazine ring and at 947 cm^{-1} assigned to C—O cyclic acetal vibration mode or C—H out-of-plane deformation [Fig. 3(a)].[37] These absorptions decreased as the curing temperature was raised from 150 to 170°C [Fig. 3(b) and (c)], and kept as a shoulder at 190°C [Fig. 3(d)] without disappearing due to the ether linkage in the backbone of the **PU** prepolymer. Meanwhile, the absorption at 2286 cm^{-1} ascribed to NCO group of **PU** prepolymer disappeared after curing at 150°C [Fig. 3(b)]. These indicate that the phenolic hydroxyl groups produced by the ring opening polymerization of **Pa** at an elevated temperature reacted with the NCO groups of **PU** prepolymer, affording a network structure.[32] The possibility of the formation of allophanate linkage by the reaction between NCO and urethane also cannot be neglected. The presence of **OMMT** was confirmed

TABLE II
DSC of PU/Pa-OMMT in case of PU/Pa = 50/50

OMMT content (wt %)	Cure condition	Exotherm		
		Onset (°C)	Max. (°C)	Quantity (cal/g)
0	Before cure	219	246	27.7
0	150°C/1h	223	252	8.9
0	170°C/1h	225	251	0.6
0	190°C/1h	231	253	0.2
1	Before cure	187	229	27.9
1	150°C/1h	192	243	7.1
1	190°C/1h	—	—	0.0
3	Before cure	158	226	28.1
3	150°C/1h	173	237	6.5
3	170°C/1h	195	247	4.3
3	190°C/1h	—	—	0.0
5	Before cure	153	223	28.8
7	Before cure	149	221	29.1
10	Before cure	145	222	27.9
20	Before cure	147	220	27.2

by the absorptions at 522 and 1048 cm^{-1} attributed to Si—O of **OMMT** that existed all the way through thermal treatments.[13]

Previous study on polybenzoxazine/clay hybrid nanocomposites revealed that the temperature needed for the ring opening polymerization of benzoxazine lowered by 30°C in the presence of **OMMT**, because of the catalytic effect of the acidic onium protons on the clay surface.[13,38] The curing behavior of **PU/Pa– OMMT** was monitored by DSC, and the results are summarized in Table II. As an example, Figure 4 illustrated the DSC profile in the case of **PU/Pa**-50/50 with 3% **OMMT** at various temperatures, along with
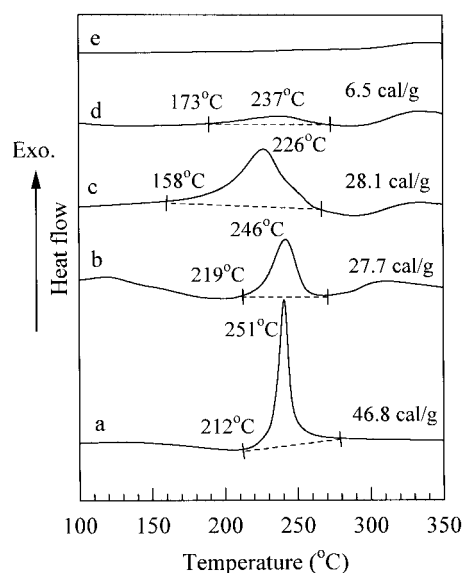

Figure 4 DSC thermograms of (a) **Pa**, (b) **PU/Pa**(50/50), and **PU/Pa**(50/50)–**OMMT** with 3% **OMMT**: (c) before cure and cured at: (d) 150°C/1 h and (e) 190°C/ 1h.
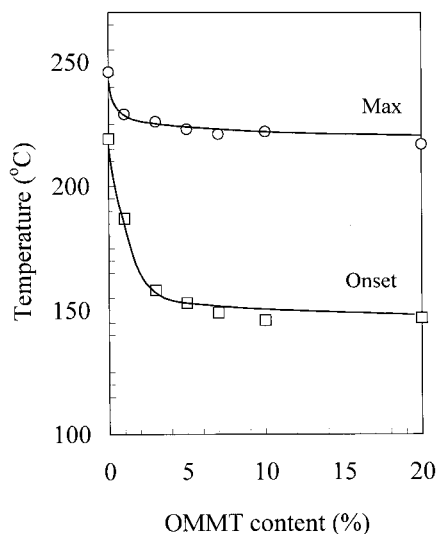
Figure 5 The effect of **OMMT** on the curing temperatures of **PU/Pa**.

pristine **PU/Pa** and **Pa**. It is clearly recognized that exothermic peak due to the ring opening of pristine **Pa** [Fig. 4(a)] remained almost the same temperature range in the case of pristine **PU/Pa** (**Fig. 4b**). But the exotherm shifted to the lower temperature range in the presence of **OMMT** [Fig. 4(c)]. In the case of **PU/Pa**-50/50 with 3% of **OMMT**, the onset of the exotherm for the nanaocomposite lowered by ca. 60°C and the maximum by 20°C compared with the pristine. The lowering tendency for both the onset and maximum temperatures of the exotherm is shown in Figure 5, which shows that relatively small amount of **OMMT** is enough to lower the cure temperature. The exothermic quantity for **PU/Pa–OMMT** decreased rapidly by the cure at 150°C for 1 h, from 28.1 down to 6.5 cal/g [Fig. 4(d)], while for the pristine **PU/Pa** decreased from 27.7 to 8.9 cal/g. After the treatments at 190°C for 1 h, exothermic peak was not found in **PU/Pa–OMMT** [Fig. 4(e)]. Because complete cure of **Pa** in the pristine **PU/Pa** was not achieved without partial degradation of **PU** component, the effectiveness of **OMMT** was clearly demonstrated for the complete cure of **Pa** in **PU/Pa** without thermally decomposing the **PU** component. As a result, the mechanical and thermal properties of **PU/Pa** were improved significantly, which will be discussed in the following sections.

Solvent resistance of PU/Pa-OMMT

The solvent resistance of **PU/Pa–OMMT** after curing at 190°C for 1 h was examined using the chosen solvents as summarized in Table III. Although the pristine **PU/Pa** films swelled in the strong polar solvent like dimethylsulfoxide (DMSO), *N,N*- dimethylform-

amide (DMF) and *N*-methyl-2-pyrrolidinone (NMP), all **PU/Pa–OMMT** films did not show any changes in all the solvents after 2 weeks immersing. The solvent resistance of **PU/Pa** was therefore improved by hybridizing with **OMMT**. This could be resulted from the outstanding barrier properties of the layered silicate structure in **OMMT** that affords a protecting wall against solvent to intrude into nanocomposite and thus protecting the material from absorbing solvent.[17,18]

Tensile properties of PU/Pa-OMMT films

The tensile properties of the **PU/Pa–OMMT** films are summarized in Table IV. The characteristics of the **PU/Pa–OMMT** films changed remarkably with the **PU/Pa** ratio and the **OMMT** content. The films changed from plastic to elastic with higher **PU** content, showing a trend similar to that of pristine **PU/Pa** films. The films also changed from elastic to plastic at a higher **OMMT** content. For example, the pristine **PU/Pa**-50/50 film was elastomer, having an elongation of more than 200%. With the **OMMT** loading, however, **PU/Pa**-50/50 films became plastic, showing increased modulus and a decreased elongation. As the content of **PU** increased up to 80%, the nanocomposite films exhibited elastic characteristics. With a higher content of **OMMT** over 10%, however, the films of **PU/Pa**-80/20 and 90/10 also became plastics, exhibiting a dramatic increase in modulus and a sharp decrease in elongation. All of these results demonstrate that **OMMT** is a remarkably effective reinforcing

TABLE III
Solubility of PU/Pa-OMMT Films[a] after Curing at 190°C/1 h

PU/Pa (wt ratio)	OMMT (wt %)	Solubility[b]					
		CHCl₃	THF	DMSO	DMF	DMAc	NMP
20/80	0	X	X	X	X	X	X
	1	X	X	X	X	X	X
	3	X	X	X	X	X	X
50/50	0	X	X	△	△	△	△
	1	X	X	X	X	X	X
	3	X	X	X	X	X	X
80/20	0	X	X	△	△	△	△
	1	X	X	X	X	X	X
	3	X	X	X	X	X	X
90/10	0	X	X	△	△	△	△
	1	X	X	X	X	X	X
	3	X	X	X	X	X	X

[a] Films were immersed in the solvents for 2 weeks.
[b] The investigated solvents were CHCl₃: Chloroform, THF: Tetrahydrofuran, DMSO: Dimethylsulfoxide, DMF: *N,N*-Dimethylformamide, DMAc: *N,N*-Dimethylacetamide, and NMP: *N*-Methyl pyrrolidine.
X: insoluble, and △: swelling.

TABLE IV
Tensile Properties of PU/Pa-OMMT Films after Curing at 190°C/1 h

Film composition					
PU/Pa (wt ratio)	OMMT (wt %)	E (MPa)	σ (MPa)	Elongation (%)	Remark
20/80	0	238	34.2	8	Plastics
	1	623	52.6	9	Plastics
	3	934	83.2	5	Plastics
50/50	0	9.82	9.6	203	Elastomer
	1	278	14.8	35	Plastics
	3	523	23.7	33	Plastics
	5	587	45.1	23	Plastics
80/20	0	5.68	3.7	343	Elastomer
	1	8.56	5.0	309	Elastomer
	3	13.1	8.3	241	Elastomer
	5	19.0	12.9	173	Elastomer
	10	217	29.3	27	Plastics
	20	243	32.3	12	Plastics
90/10	0	3.42	2.4	505	Elastomer
	1	5.23	3.3	453	Elastomer
	3	7.81	5.7	354	Elastomer
	5	7.59	5.9	192	Elastomer
	10	121	13.1	36	Plastics
	20	163	18.4	18	Plastics

agent because of the good interactions between the silicate layers and **PU/Pa** matrix.

Both the tensile modulus and strength of **PU/Pa** were remarkably increased by the introduction of **OMMT**. Tensile modulus of **PU/Pa** films is plotted against **OMMT** content in Figure 6, which clearly shows that tensile modulus increases with a higher **OMMT** content. Please notice that modulus is shown in a logarithm scale. A leap-up increase was observed for the films with 80/20 and 90/10 of **PU/Pa** ratios. This is considered to result from the change of the film characteristics from elastomer to plastic as **OMMT** content increased over 10%. Tensile modulus of the plastic films was above 100 MPa, and that of the
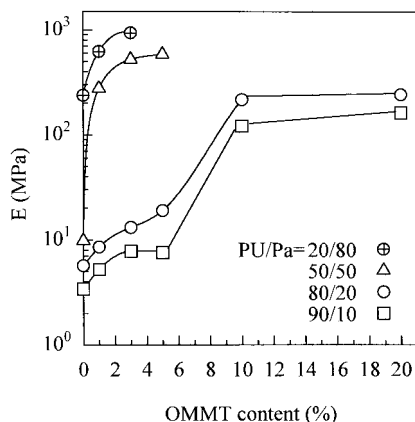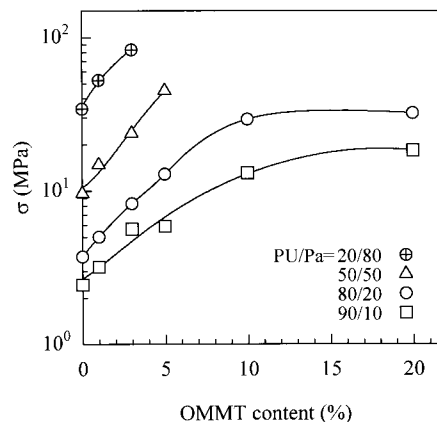

Figure 7 The effect of **OMMT** on the tensile strength of **PU/Pa**.

elastomer films was below 20 MPa. The tensile strength of **PU/Pa** films also increased with **OMMT** content, as shown in Figure 7. The increase was prominent up to 10% of clay loading, and was moderate above 10%. The elongation at break, on the other hand, decreased with **OMMT** content.

Figure 8 shows examples of stress–strain curves for the elastomer films in the case of **PU/Pa**-80/20 with various **OMMT** content. We clearly see that, with the increase of clay content, tensile modulus and tensile strength increased, while elongation decreased. The results may be considered to be due to the remarkable reinforcing effect of **OMMT** because of good interaction between the silicate layer and the **PU/Pa** matrix, and also due to the network structure of PU/Pa,[32] which stiffened the macromolecular chain of the nanocomposite.

Dynamic mechanical analysis (DMA) of PU/Pa–OMMT

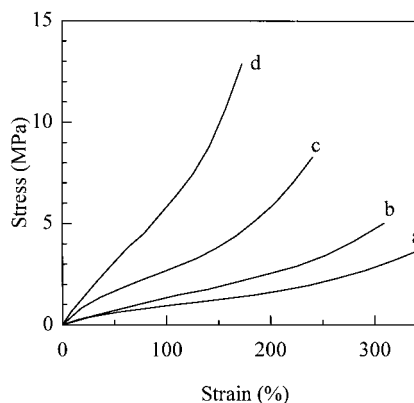The viscoelastic properties of **PU/Pa–OMMT** from DMA are summarized in Table V. There is a clear

Figure 6 The effect of **OMMT** on the tensile modulus of **PU/Pa**.

Figure 8 Stress–strain curves of elastomer films for **PU/Pa**-80/20 with the content of **OMMT**: (a) 0%, (b) 1%, (c) 3%, and (d) 5%.

TABLE V
Viscoelastic Properties of PU/Pa-OMMT Films after Curing at 190°C/1 h

PU/Pa (wt ratio)	OMMT (wt %)	E' (GPa) at		T_g (°C) from		Remark
		$-50°C$	$25°C$	E'' max.	tan δ	
20/80	0	6.12	3.22	27	43	Plastic
	1	6.58	3.26	38	66	Plastic
	3	7.06	4.13	39	75	Plastic
	5	7.07	4.66	40	81	Plastic
50/50	0	3.82	4.85×10^{-3}	−1	7	Elastic
	1	4.97	1.12	11	27	Plastic
	3	6.13	1.26	15	56	Plastic
	5	5.89	1.31	16	71	Plastic
80/20	0	3.07	2.07×10^{-3}	−25	−6	Elastic
	1	3.56	2.81×10^{-3}	−12	2	Elastic
	3	4.17	17.0×10^{-3}	−10	14	Elastic
	5	5.62	24.2×10^{-3}	−8	21	Elastic
	10	5.28	39.1×10^{-3}	−2	30	Plastic
	20	6.32	0.15	0	33	Plastic
90/10	0	1.42	2.02×10^{-3}	−35	−10	Elastic
	1	3.23	2.15×10^{-3}	−26	−3	Elastic
	3	4.21	6.47×10^{-3}	−23	8	Elastic
	5	4.59	12.6×10^{-3}	−22	17	Elastic
	10	4.86	28.9×10^{-3}	−14	22	Plastic
	20	5.01	0.16	−11	23	Plastic

tendency that storage modulus (E') of **PU/Pa–OMMT** films increased as the content of **OMMT** increased, which agreed well with tensile properties as mentioned above.

The examples of the viscoelastic properties for plastic films are shown in Figure 9 in the case of PU/Pa = 20/80. It was clearly shown that, with the increase of **OMMT** content, storage modulus increased, T_g shifted to a higher temperature, and damping was suppressed.

The examples of the viscoelastic properties for elastomer films are shown in Figure 10 in the case of **PU/Pa** = 80/20, which also shows that, with the increase of **OMMT** content, storage modulus increased, T_g shifted to a higher temperature, and damping was
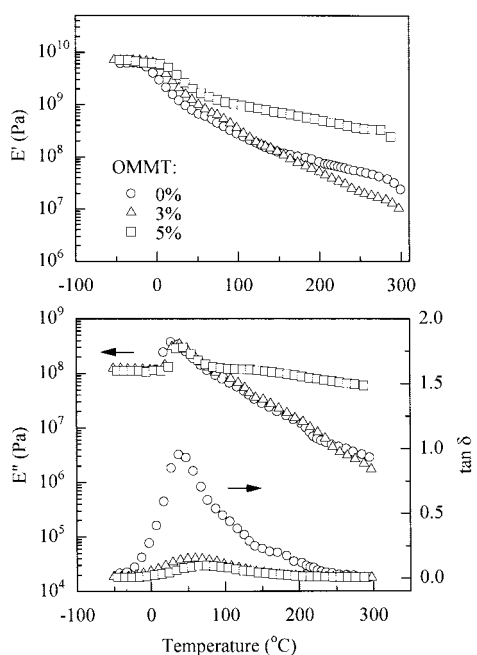

Figure 9 Viscoelastic properties of **PU/Pa**(20/80)–**OMMT** plastic films.
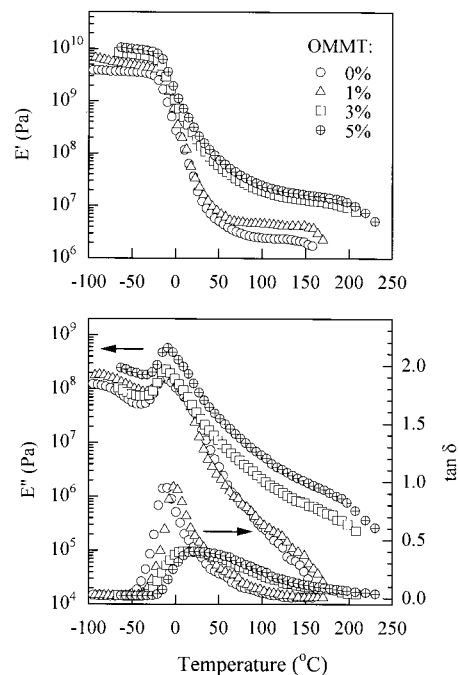

Figure 10 Viscoelastic properties of **PU/Pa**(80/20)–**OMMT** elastomer films.
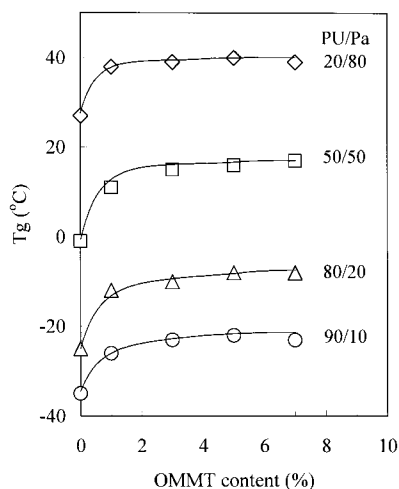
Figure 11 The effect of **OMMT** content on the T_gs of **PU/Pa** obtained from E' max.

TABLE VI
Thermal Stability of PU/Pa-OMMT Films after Curing at 190°C/1 h[a]

PU/Pa (wt ratio)	OMMT (wt %)	Temperature (°C) at	
		5 wt % loss	10 wt % loss
20/80	0	268	302
	1	298	336
	3	301	342
	5	302	349
50/50	0	259	281
	1	286	322
	3	291	348
	5	293	356
80/20	0	256	282
	1	284	321
	3	288	320
	5	289	322
	10	294	341
	20	297	346
90/10	0	255	286
	1	277	316
	3	281	327
	5	282	326
	10	287	325
	20	290	331

[a] From TGA.

suppressed. It is especially to be noted, in the case of elastomer films, that the rubbery plateau regions prolonged up to higher temperature. The rubbery plateau region reached ca. 230°C at 5% of **OMMT** content, which is ca. a 70°C increase from the pristine one. It is therefore concluded that the thermomechanical property of **PU/Pa** is enhanced by **OMMT**, which may come from a good reinforcement of **PU/Pa** by **OMMT**.

DMA also allows the determination of T_g of **PU/Pa–OMMT** from the maximum of loss modulus (E'') or tan σ. As shown in Figures 9 and 10, only one T_g was observed for all the **PU/Pa–OMMT** films from both E'' and tan δ. It was also observed, as shown in Figure 11, that T_g values from E'' maximum shifted to higher temperatures with the increase of **OMMT** content, although the increase was not so much above 2% of the **OMMT** content. It is therefore considered that **PU** and polybenzoxazine are well miscible due to the *in situ* copolymerization of **Pa** and **PU** prepolymer, as mentioned above. In other words, a homogenous phase is induced by *in situ* copolymerization.

Thermal stabilities of PU/Pa–OMMT

The thermal stabilities of **PU/Pa–OMMT** were investigated by TGA. Results are summarized in Table VI, and typical TGA profiles are shown in Figure 12. It is evidently found that the initial decomposition temperatures (defined at 5 and 10% weight loss temperatures) of **PU/Pa** were enhanced by hybridizing with **OMMT**, while the pristine **PU/Pa** showed almost the same at any ratio of **PU/Pa**.

The dependence of the temperatures at 5% weight loss on **OMMT** loading is shown in Figure 13. It was proved that the thermal stability of **PU/Pa** was notably improved by incorporating even a very small amount of **OMMT**. The decomposition temperatures are thus

increased sharply with lower content, but dully with higher content of **OMMT**. This phenomenon, similar with those of polybenzoxazine/clay[13] and polyimide/clay nanocomposites,[19] may be due to aggregation of **OMMT** at a high loading. The improvement of the thermal stabilities of **PU/Pa** by hybridizing **OMMT** was suggested to be based on two major points. First, the layered silicates of **OMMT** make the path longer for escaping of the thermally decomposed volatiles. In other words, part of the thermally decomposed volatiles is captured by **OMMT**.[16] Second, the crosslink density of **PU/Pa** in the presence of **OMMT** is higher than that of pristine **PU/Pa** due to the efficient cure of
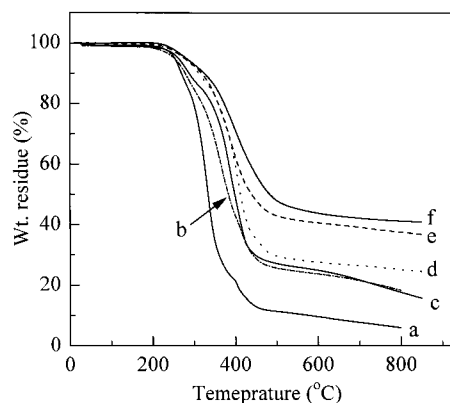

Figure 12 TGA of the pristine **PU/Pa** of (a) 90/10 and (b) 80/20; and **PU/Pa–OMMT** with 1% **OMMT** in the ratios of (c) 90/10, (d) 80/20, (e) 50/50, and (f) 20/80/
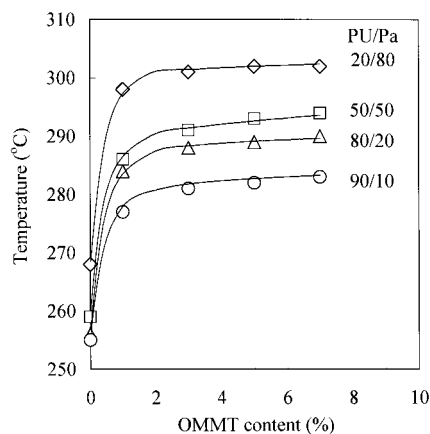
Figure 13 The effects of the **OMMT** on decomposition temperatures of **PU/Pa**.

Pa from the catalytic effect of **OMMT** on the ring-opening polymerization,[13] which could lead to improved thermal stability.

CONCLUSIONS

A series of **PU/Pa–OMMT** films were successfully prepared using solvent method by the *in situ* copolymerization of **PU** prepolymer and **Pa** in the presence of **OMMT**. **PU/Pa–OMMT** films obtained by the thermal cure at 190°C were deep yellow and transparent. Exfoliated structure was achieved in the case of less than 5% of **OMMT** loading, a mixed or intercalated configuration in the case of more than 7% of **OMMT** loading. The temperature necessary for the curing of **PU/Pa** was lowered by hybridizing with **OMMT** due to the catalytic effect of clay surface on the ring-opening polymerization of **Pa**, which enabled complete cure of **Pa** without thermally decomposing **PU** component. **PU/Pa–OMMT** showed superior solvent resistances to pristine **PU/Pa**. **PU/Pa–OMMT** films exhibited plastic or elastomer characteristics depending on the **PU/Pa** ratio and **OMMT** content. The tensile strength and modulus of the **PU/Pa** films increased remarkably, while the elongation decreased with the increase of **OMMT** loading. The distortion temperature of **PU/Pa–OMMT** was higher than that of pristine **PU/Pa**. The thermal stabilities of **PU/Pa** were improved significantly by hybridizing with even a small amount of **OMMT**.

References

1. Manson, J. A.; Sperling, L. H. Polymer Blends and Composites; Plenum: New York, 1976.
2. Nielsen, L. E. Mechanical Properties of Polymer and Composites; Marcel Dekker: New York, 1974, vol. 2.
3. Okada, A.; Usuki, A.; Kurauchi, T.; Kamikaito, O. In Hybrid Organic–Inorganic Composites; Mark, J. E.; Lee, C. Y. C.; Bianconi, P. A., Eds.; American Chemical Society: Washington, DC, 1995.
4. Giannelis, E. P. In Biomimetic Mater Chem; Mann, S., Ed.; VCH: New York, 1996.
5. LeBaron, P. C.; Wang, Z.; Pinnavaia, T. J. Appl Clay Sci 1999, 15, 11.
6. Okada, A.; Fukushima, Y.; Kawasumi, A.; Inagaki, S.; Usuki, A.; Sgiyama, S.; Kurauchi, T. Kamikaito, O. U.S. Pat. 4,739,007 (1988).
7. Okada, A.; Kawasumi, A.; Usuki, A.; Kojima, Y.; Kurauchi, T.; Kamikaito, O. Mater Res Soc Proc 1990, 171, 45.
8. Messersmith, P. B.; Giannelis, E, P. Chem Mater 1994, 6, 1719.
9. Lan, T.; Kaviratna, P. D.; Pinnavaia, T. J. Chem Mater 1995, 7, 2144.
10. Wang, A.; Pinnavaia, T. J. Chem Mater 1998, 10, 1820.
11. Kormann, X.; Lindberg, H.; Berglund, L. A. Polymer 2001, 42, 1303.
12. Kormann, X.; Berglund, L. A.; Sterte, J. Polym Eng Sci 1998, 38, 1351.
13. Agag, T.; Takeichi, T. Polymer 2000, 41, 7083.
14. Magaraphan, P. P. R.; Ishida, H. Mater Res Innovat 2001 4, 187.
15. Kim, G. M.; Lee, D. H.; Hoffmann, B.; Kressler, J.; Stöppelmann, G. Polymer 2001, 42, 1095.
16. Yano, K.; Usuki, A.; Okada, A.; Kurauchi, T.; Kamigaito, O. J Polym Sci Polym Chem 1993, 31, 2493.
17. Yano, K.; Usuki, A.; Okada, A. J Polym Sci Polym Chem 1997, 35, 2289.
18. Yang, Y.; Zhu, Z.; Yin, J.; Wang, X.; Qi, Z. Polymer 1999, 40, 4407.
19. Agag, T.; Koga, T.; Takeichi, T. Polymer 2001, 42, 3399.
20. Huang, J. C.; Zhu, Z. K.; Yin, J.; Qian, X. F.; Sun, Y. Y. Polymer 2001, 42, 873.
21. Galgali, G.; Ramesh, C.; Lele, A. Macromolecules 2001, 34, 852.
22. Laus, M.; Francescangeli, O.; Sandrolini, F. J Mater Res 1997, 12, 31314.
23. Wang, A.; Pinnavaia, T. J. Chem Mater 1998, 10, 3769.
24. Chen, T. K.; Tien, Y. I.; Wei, K. H. J Polym Sci Polym Chem 1999, 37, 2225.
25. Zilg, C.; Thomann, R.; Mülhaupt, R.; Finter, J. Adv Mater 1999, 11, 49.
26. Chen, T. K.; Tien, Y. I.; Wei, K. H. Polymer 2000, 41, 1345.
27. Xu, R.; Manias, E.; Snyder, A. J.; Runt, J. Macromolecules 2001, 34, 337.
28. Okamoto, M.; Morita, S.; Taguchi, H.; Kim, Y. H.; Kotaka, T.; Tateyama, H. Polymer 2000, 41, 3887.
29. Okamoto, M.; Morita, S.; Kim, Y. H.; Kotaka, T.; Tateyama, H. Polymer 2001, 42, 1201.
30. Zanetti, M.; Camino, G.; Thomann, R.; Mülhaupt, R. Polymer 2001, 42, 4501.
31. Takeichi, T.; Guo, Y.; Agag, T J Polym Sci Polym Chem 2000, 38, 4165.
32. Takeichi, T.; Guo, Y. Polym J 2001, 33, 437.
33. Agag, T.; Takeichi, T.; Toda, H.; Kobayashi, T. Int J Mater Product Technol 2001, 2, 706.
34. Zuo, M.; Takeichi, T. J Polym Sci Polym Chem 1997, 35, 3745.
35. Zuo, M.; Qian, X.; Takeichi, T. Polymer 1998, 39, 6883.
36. Zuo, M.; Takeichi, T. Polymer 1999, 40, 5153.
37. Wang, Y.-X.; Ishida, H. Macromolecules 2000, 33, 2839.
38. Wang, Y. X.; Ishida, H. Polymer 1999, 40, 4563.